

Three-Dimensional Electromagnetic Field Calculation for Microwave Holography

Mayuko KOGA, Ryota TAKENAKA, Hayato TSUCHIYA^{1,a)}, Ryo MANABE, Naofumi IWAMA¹⁾, Shuji YAMAMOTO²⁾ and Soichiro YAMAGUCHI²⁾

University of Hyogo, Himeji 671-2280, Japan

¹⁾*National Institute for Fusion Science, Toki 509-5292, Japan*

²⁾*Kansai University, Suita 564-8680, Japan*

(Received 21 August 2020 / Accepted 4 March 2021)

The lens-less technique of microwave holography is expected to provide information of three-dimensional structures of plasma with a wide field of view. From the complex amplitudes of waves, which are observed on a single planar array of antennas, we will be able to obtain an imaging of the three-dimensional object. With a geometry of back-scattering observation, the feasibility is examined with a numerical tool of electromagnetic analysis on dielectric objects. With respect to the variety of the dielectric constant and shape of object, it is shown that useful information can be acquired in regarding the complex amplitude distribution at planar detector.

© 2021 The Japan Society of Plasma Science and Nuclear Fusion Research

Keywords: microwave holography, lens-less imaging, reflectometer, electromagnetic field calculation

DOI: 10.1585/pfr.16.1402063

1. Introduction

The microwave holography has application possibility in various fields of scientific research. In the mode of digital holography for image formation, it is a lens-less technique in current progress [1, 2], which is attractive for fusion plasma study. In plasma confinement studies, the measurement of turbulence is important. Three-dimensional (3D) imaging with a single and wide field of view would be effective to investigate the physics of non-linear dynamical phenomena such as turbulence. A lens-less method of microwave holography has been proposed for this purpose [3]. The microwave holography using the multi-channel heterodyne detection to obtain amplitudes and phases of the observed wave is suitable to capture the plasma density structure caused by turbulence. If such a lens-less system is implemented instead of the conventional systems of plasma imaging [4–8], the field of view will be well extended.

In Ref. [3], observations were theoretically produced under the assumptions of spherical wave transmission and scattering with the Born approximation, and the image reconstruction was successful in numerical simulation. In this paper, feasibility study of electromagnetic field calculation is progressed in revealing the complex amplitudes which will be observed in actual experiments. Electromagnetic field calculation is adopted to predict the complex amplitude distributions that should be observed on a planar array of antennas with respect to various dielectric targets. The target is changed in not only the shape but also

the dielectric constant, that is, from the value so low that Born-approximation based methods of image reconstruction may be applicable and to the value so high that the scattering is nearly the surface reflection. After the holographic inversion is briefly reviewed, the results of calculation are exhibited.

2. Microwave Holography

Figure 1 shows the schematic diagram of microwave holography. A microwave (RF) is emitted from the source position $\mathbf{p}_s = (x_o, y_o, z_o)$ and injected to a target. The spa-

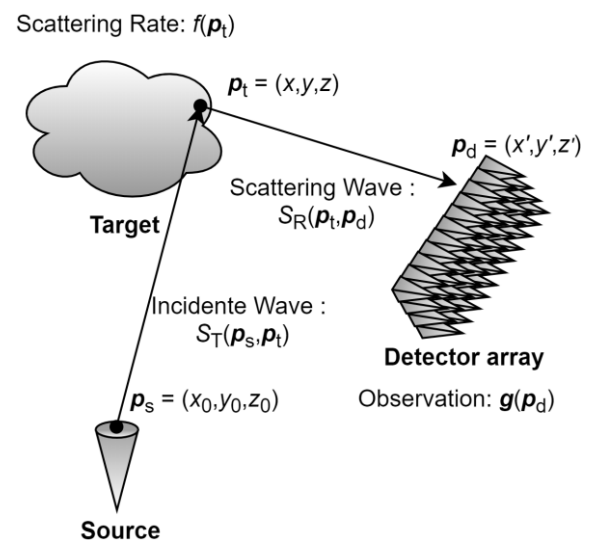


Fig. 1 Schematic diagram of microwave holography.

author's e-mail: koga@eng.u-hyogo.ac.jp

^{a)} Present affiliation: Kawasaki Heavy Industry

tial distribution of scattering rate on the target is denoted as $f(\mathbf{p}_t)$. The wave scattered from the target position $\mathbf{p}_t = (x, y, z)$ reaches the detector at a position $\mathbf{p}_d = (x', y', z')$. When the incident wave can reach the scattering points without any perturbation, the elemental of complex amplitude of the wave propagating along the path of \mathbf{p}_s , \mathbf{p}_t and \mathbf{p}_d , is expressed as

$$S_{std} = S_T(\mathbf{p}_s, \mathbf{p}_t) f(\mathbf{p}_t) S_R(\mathbf{p}_t, \mathbf{p}_d), \quad (1)$$

where $S_T(\mathbf{p}_s, \mathbf{p}_t)$ and $S_R(\mathbf{p}_t, \mathbf{p}_d)$ are functions which describe the wave propagation from \mathbf{p}_s to \mathbf{p}_t and from \mathbf{p}_t to \mathbf{p}_d , respectively. Because the actual measurement $g(\mathbf{p}_d)$ is the complex amplitude of the electric field that is a superposition of waves reflected from all the points of the target, $g(\mathbf{p}_d)$ is expressed as a volume integration of $S_{std} d\mathbf{p}_t$. When the detector elements and the voxels of target are indexed with m and n , the integration is approximated as a sum

$$\begin{aligned} g_m &= \sum_{n=1}^N S_{std} d\mathbf{p}_t \\ &= \sum_{n=1}^N h_{mn} f_n \quad (m = 1, 2, \dots, M), \end{aligned} \quad (2)$$

where the adopted coefficients h_{mn} depend on the configuration of the source, the target and the detector; M and N are the numbers of detector elements and target voxels, respectively.

Adopting a matrix H with elements h_{mn} and the vector representations of f_n and g_m , we rewrite Eq. (2) as

$$Hf = g, \quad (3)$$

which is a linear equation to be solved for the target image f . When the dielectric constant of the target is so low that the Born approximation holds in scattering, the coefficient matrix H can be derived by applying the above consideration to the actual system with knowledge of $S_T(\mathbf{p}_s, \mathbf{p}_t)$ and $S_R(\mathbf{p}_t, \mathbf{p}_d)$. Even in such a case, when dielectric targets are employed for a substitution of plasmas, the H and also the observation g are not easily derived because of eddy currents in the target surface etc. In the following analysis, however, the value of the dielectric constant is extensively changed for the purpose of examining the sensitivity of the assumed observation system.

3. Method of Calculation

3.1 Electromagnetic field analysis software

In order to obtain electric field profile on the detector plane, electromagnetic field calculation was performed by the moment method and the high-speed multipole method using the electromagnetic field analysis software Efield (Advanced Technology Co., Ltd.). When the number of calculation points was small, the moment method was used. Otherwise the fast multipole method was used. The software Efield is capable of 3D electromagnetic simulations in both time and frequency domains. It was used in the frequency domain in this paper.

3.2 Specifications of PC

The PC specifications used in this study are as follows.

OS	Windows 10 Pro
CPU	Intel (R) Xeon (R) CPU X5690 @ 3.47 GHz (2 processors)
Memory	192 GB
System type	64-bit operating system

Computation time depends on the fineness of the computational domain. The calculation time was 2 - 100 minutes for each model in the condition of 2 - 5 mm in mesh size.

4. Simulations by Electromagnetic Field Calculation

4.1 Reflected waves when the shape of the target is changed

The calculation model is shown in Fig. 2. We set the origin as the center of gravity of the target. The microwave source is 30 mm × 20 mm in size and assumed as the edge of a rectangular waveguide, and the detector plane is wide as 500 mm × 500 mm. In order to investigate overall image of the electric field, we set more than enough large detector plane. The microwave is transmitted at a fixed frequency of 30 GHz and with the electric field distribution of TE₁₀ mode on the source. The distance from the microwave source to the dielectric target is 100 mm while the distance from the dielectric target to the detector plane is 110 mm. The reflection angle is 30 degrees.

In order to see how the electric field distribution in the detector plane changes with the shape of target, we calculated for some dielectric targets. Figure 3 illustrates the examined dielectric targets: (1) 40 mm diameter ball, (2) 40 mm cube, (3) two 40 mm cubes (aligned on Y-axis), (4) two 40 mm cubes (aligned on X-axis), (5) two 40 mm cubes (aligned on Z-axis), (6) cylinder 40 mm in diameter

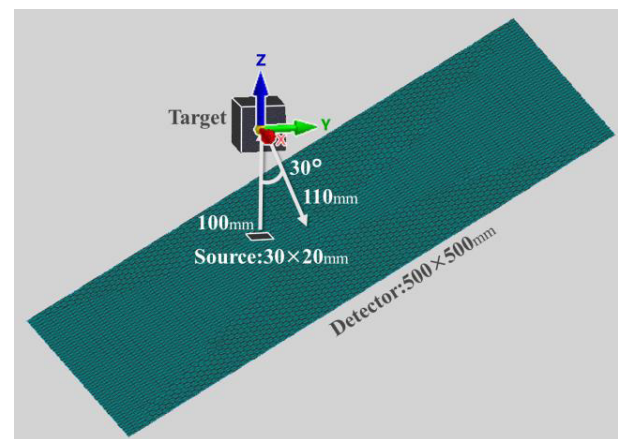


Fig. 2 Calculation model.

and 40 mm in height. All dielectric targets have a dielectric constant of 2.3.

The free boundary was set in the far field and the medium except for the target was set to be vacuum. In these conditions, we calculated the complex amplitude of microwave passing the detection point on the detector plane in vacuum. The dominant polarization direction of

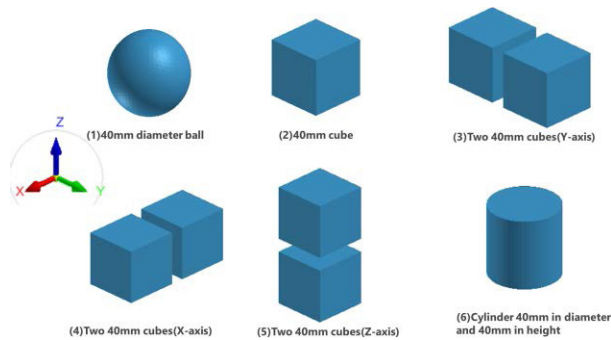


Fig. 3 3D illustration of the examined dielectric targets. (1) 40 mm diameter ball, (2) 40 mm cube, (3) two 40 mm cubes (aligned on Y-axis), (4) two 40 mm cubes (aligned on X-axis), (5) two 40 mm cubes (aligned on Z-axis), (6) cylinder 40 mm in diameter and 40 mm in height.

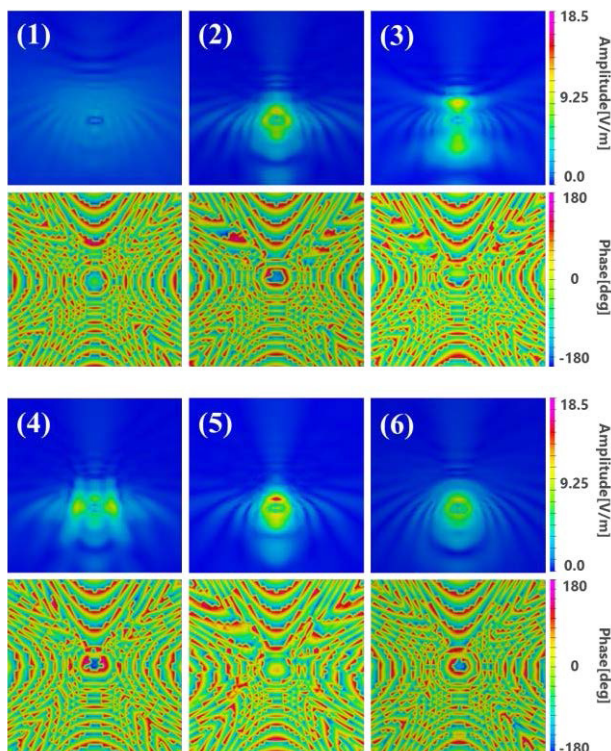


Fig. 4 Amplitude/phase distribution of the reflected wave with different shapes and alignments of the target. (1) 40 mm diameter ball, (2) 40 mm cube, (3) two 40 mm cubes (aligned on Y-axis), (4) two 40 mm cubes (aligned on X-axis), (5) two 40 mm cubes (aligned on Z-axis), (6) cylinder 40 mm in diameter and 40 mm in height.

microwave through the detector plane was expected to be along to y axis, which was determined by TE_{10} mode in the source. Because we assumed to use a horn antenna with y direction sensitivity in electric field for a detector, we show and discuss only y directional components of electric field in this paper. The results are shown in Fig. 4. The amplitude of the electric field from the target (1) is small in comparison to other cube models due to the all-round scattering by the spherical surface. In the case of two cubes, the amplitude distribution changes with the direction of alignment. The observation is sensitive also to the change into a cylinder. These results show that the observed amplitude distribution contains 3D morphological information of targets, suggesting that not only the phase but also the amplitude of the electric field are useful for image reconstruction.

4.2 Reflected wave when the dielectric constant of the target is changed

In order to investigate the available range of the dielectric constant of the target, the complex amplitude distribution was calculated and examined for the variation of the dielectric constant. Concerning the test scheme of holography in Sec. 4.1, the target was replaced by a cuboid (200 mm × 200 mm × 40 mm) and changed extensively in dielectric constants as follows: (1) 2.3, (2) 23, (3) 230, (4) 2300, (5) 23000, (6) 230000. As a reference, for example,

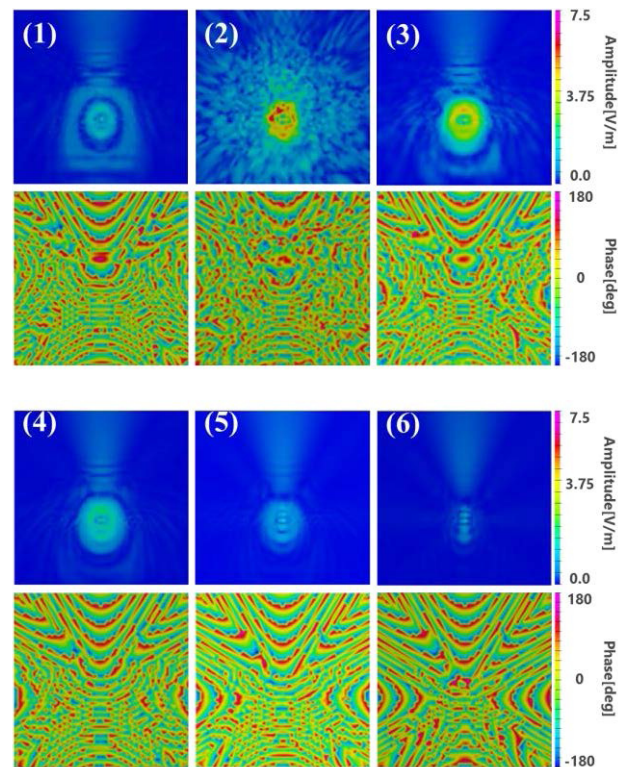


Fig. 5 Amplitude/phase distribution of the reflected wave with different dielectric constants of the target. (1) 2.3, (2) 23, (3) 230, (4) 2300, (5) 23000, (6) 230000.

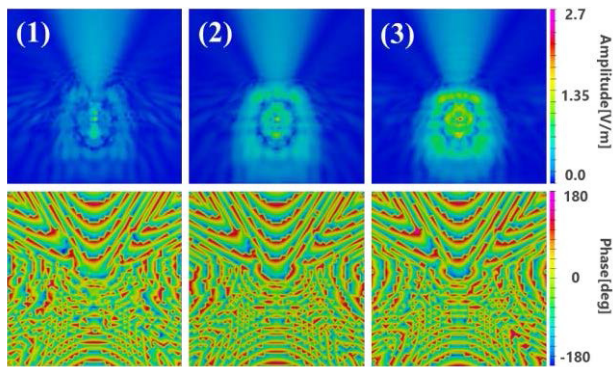


Fig. 6 Amplitude/phase distribution of the reflected wave with different thicknesses of the target, (1) 10 mm, (2) 30 mm, (3) 50 mm.

ethyl alcohol has a dielectric constant of 23 and cork has a dielectric constant of 2.3.

Figure 5 shows the results. In Figs. 5 (4), (5), (6) with dielectric constants above 2300, the microwave is scattered mostly at the surface of the target and does not penetrate to the inside. The measurement is similar to the reflectometry. In contrast, in Figs. 5 (1), (2), (3) with dielectric constants around 2.3 - 230, there is an effect of the scattering from inside, and the electric field pattern changes with a remarkable increase of emission intensity.

4.3 Reflected wave when the thickness of the dielectric target is changed

In order to ascertain the possibility of reconstructing 3D objects from the observation from a single field of view, we changed the thickness of the dielectric target as 10 mm, 30 mm, 50 mm along the z-axis, while keeping the bottom area of the target (100 mm \times 100 mm) and the dielectric constant (2.3).

Figure 6 shows the results. With the increase of thick-

ness, the amplitude of the electric field becomes larger, as expected, because the back-scattering inside the target is increased. The 2D data obtained in a single direction reflects the 3D structure of the target.

5. Summary

The complex amplitude profile on a plane with wide range and high resolution which could not be obtained in actual experiment was calculated by using three-dimensional electromagnetic field calculation. Changing the shape and the alignment of targets, the complex amplitude profiles on the detector plane seem to be affected by both surface reflectance and internal scattering. Changing the dielectric constant of the target, they seem to be affected by the amount of internal scattering. These facts indicate that observed complex amplitude profiles on the detector plane reflects information of three-dimensional targets, that is, it is suggested the possibility of a three-dimensional image reconstruction by observed data from a single field of view. These findings will be useful not only for plasma measurements but also for measurements of other dielectrics.

Acknowledgments

This work is performed with the support and under the auspices of the NIFS Collaboration Research program (NIFS18KLEP029).

- [1] B. Sun *et al.*, *Science* **340**, 844 (2013).
- [2] J. Wu *et al.*, *Light: Science & Applications* **9**, 53 (2020).
- [3] H. Tsuchiya *et al.*, *Plasma Fusion Res.* **14**, 3402146 (2019).
- [4] T. Munsat, E. Mazzucato and H. Park, *Rev. Sci. Instrum.* **74**, 1426 (2003).
- [5] S. Yamaguchi *et al.*, *Rev. Sci. Instrum.* **77**, 10E930 (2006).
- [6] W. Lee *et al.*, *JINST* **7**, C01070 (2012).
- [7] M. Muscatello *et al.*, *Rev. Sci. Instrum.* **85**, 11D702 (2014).
- [8] H. Tsuchiya *et al.*, *Plasma Fusion Res.* **13**, 3402063 (2018).